Mechanistic Study on Electrochemical Reduction of Calix[4]quinone in Acetonitrile Containing Water§

Young-Ok Kim,† Young Mee Jung,† Seung Bin Kim,† Byung Hee Hong,‡ Kwang S. Kim,*,‡ and Su-Moon Park*,†

Department of Chemistry and Center for Integrated Molecular Systems, and National Creative Research Initiative Center for Superfunctional Materials, Pohang University of Science and Technology, Pohang 790-784, Korea (ROK)

Received: January 11, 2004; In Final Form: February 18, 2004

The mechanism of electrochemical reduction of calix[4]quinones (CQs) is of vital importance, as their reduction products, calix[4]hydroquinones (CQH_8s), are known to self-assemble organic nanotubes, which in turn self-assemble novel metal nanostructures by a self-synthetic process of electrochemical reduction of solvated metals. We therefore conducted detailed studies of electrochemical reduction of CQ in rigorously dried acetonitrile (CH_3CN) and in CH_3CN containing varied amounts of water as well as perchloric acid. CQ undergoes a series of reversible one electron reductions in dry CH_3CN leading to anion radicals of each of *p*-benzoquinone units followed by formation of dianions. However, a series of following chemical-electrochemical reactions with protons takes place after the initial electron transfer in CH_3CN containing water. The final product of this series of reactions is identified as CQH_8 via an eight electron, eight proton reaction. The intermediate species are identified, and the reaction mechanism is elucidated using transient electrochemical, electrochemical quartz crystal microbalance and spectroelectrochemical measurements. The present results could be utilized to fine control the self-assembling reaction of nanotubes by electrochemical processes and to design electrochemically controllable nanomechanical devices.

Introduction

Calixarenes have received much attention due to their ability to bind ions or molecules, acting as a receptor molecule for the host−guest complexes.[1] Electroactive calixarenes could be more attractive because their electroactive groups including quinone[2] or nitroaromatic moieties[3] provide chemists with opportunities to control the binding ability as well as the chemical selectivity. The electrochemical control of binding properties for guest molecules may lead to applications otherwise unavailable in chemical and biochemical reaction systems.

It is known that CQH_8, one of the redox active calixarenes with four hydroquinone moieties, forms self-assembled organic nanotube bundles.[4] Ultrathin silver wires of a diameter of 0.4 nm were shown to grow inside the CQH_8 nanotubes under ambient aqueous conditions when silver nitrate is added to the aqueous solution containing the nanotubes. Metal, semiconductor, or conductive polymer nanowires have been studied extensively due to their possible uses in manufacturing nanoscale devices.

Electrochemical reduction of CQ can be thought of as four consecutive reductions of *p*-benzoquione (*p*-BQ) units as CQ is made of four *p*-BQs connected in parallel by four $-CH_2-$ groups in between. *p*-BQ undergoes reversible two one-electron transfer reductions to form anion radicals and dianions in rigorously dried nonprotic solvents.[5] However, the mechanism of *p*-BQ reduction may be summarized as follows in aqueous solutions:[6]

$$Q + e^- \rightleftharpoons Q^{-\bullet} \quad (1)$$

$$Q^{-\bullet} + H^+ \rightleftharpoons QH^\bullet \quad (2)$$

$$QH^\bullet + e^- \rightleftharpoons QH^- \quad (3)$$

$$QH^- + H^+ \rightleftharpoons QH_2 \quad (4)$$

where Q represents *p*-BQ. The sequence of the reactions is thus described as two rounds of an electron-transfer coupled with a chemical reaction, i.e., the ECEC or EHEH mechanism, unless *p*-BQ is reduced further to its dianion, Q^{2-}, in the absence of protons. When the acidity of the medium is high, reactions 2 and 4 can be so fast that the whole reaction may be described as a concerted two-electron, two-proton reaction

$$Q + 2H^+ + 2e^- \rightleftharpoons QH_2 \quad (5)$$

where QH_2 is 1,4-dihydroquinone. This reaction is the basis of what is known as a "quinone/hydroquinone electrode" for pH measurements.

Now the electrochemistry of CQ in rigorously dried nonaqueous solutions would most likely be expected to follow the reactions summarized above. In other words, CQ would undergo four consecutive reversible one-electron reductions to form anion radicals of each *p*-BQ unit, followed by the formation of dianions in dry nonprotic solvents. In aqueous solutions,

* To whom correspondence should be addressed. E-mail: smpark@postech.edu. Phone: +82-54-279-2102. Fax: +82−54−279−3399.
† Department of Chemistry and Center for Integrated Molecular Systems.
‡ National Creative Research Initiative Center for Superfunctional Materials.
§ Dedicated to the occasion of Professor Dong Han Kim's retirement.

10.1021/jp049864n CCC: $27.50
Published on Web 03/20/2004

however, the sequence summarized above as reactions 1 through 4 or 5 would be observed depending on the acidity of the medium.

Recently, electrochemical studies of CQ in nonaquous media including CH_3CN,[7] *N*,*N*-dimethylformamide (DMF),[8] and dichloromethane (CH_2Cl_2)[9] have been reported. All of these experiments were conducted under an argon or nitrogen atmosphere in rigorously dried solvents to remove residual water, and indeed its electrochemistry in these media was described as the formation of anion radicals of four *p*-BQ units before the formation of dianions. Removal of water ensures the stability of intermediate species such as anion radicals and/or dianions. However, the electrochemistry of CQ in aqueous media should be important just as well because CQH_8 would be formed as a final product upon reducing CQ in aqueous media. Further, CQH_8 is known to form organic nanotubes in aqueous media under appropriate conditions.[4b] Water must play an important role in making organic nanotube bundles by four hydrogen bonds between OH groups of hydroquinone moieties and water molecules. For this reason, our present study addresses electrochemical reduction of CQ to CQH_8 in solutions containing water, primarily aiming at elucidation of the reaction mechanism involved in electrochemical reduction of CQ to CQH_8 employing transient electrochemical, electrochemical quartz crystal microbalance (EQCM), and spectroelectrochemical techniques, and its relevance to the formation of CQH_8 nanotubes upon CQ reduction is discussed. Thus, we conducted experiments in rigorously dried CH_3CN first as a control experiment, followed by a series of experiments, in which varied amounts of water and proton sources were used.

Experimental Method

CQ and CQH_8 were synthesized and purified according to the procedure described in the literature.[10] CH_3CN (Aldrich, 99.8%, anhydrous) was purified by three successive vacuum distillations over P_2O_5 to remove organic impurities and water. Tetrabutylammonium hexafluorophosphate ($TBAPF_6$, Aldrich, $\geq$ 99.0%) was recrystallized twice from absolute ethanol and dried overnight under reduced pressure at 100 °C. After oxygen was removed, the solvent and the supporting electrolyte were moved to a glovebox under an argon atmosphere. CQ was dried at 100 °C under vacuum overnight. Acetonitrile was dried by three freeze−pump−thaw cycles under vacuum. In some experiments, where the water−CH_3CN mixed solvent was used, twice-distilled deionized water was used. In these cases, the solution was bubbled with argon or nitrogen to remove oxygen. The supporting electrolyte was mostly 0.10 M $LiClO_4$ (Aldrich, 99.99%) unless otherwise stated.

Electrochemical experiments were performed using an EG&G PAR model 273-A potentiostat/galvanostat. Glassy carbon and gold disk (area = 0.20 cm^2) electrodes used as a working electrode were polished successively with 1.0, 0.3, and 0.05 μm alumina slurries (Fisher) and cleaned by ultrasonication in doubly distilled, deionized water before drying for use. The platinum spiral wire and Ag/AgCl (or Ag wire) were used as counter and reference electrodes, respectively.

The EQCM experiments were carried out using an EG&G-Seiko model 917 quartz crystal analyzer (QCA) along with an EG&G PAR model 273 A potentiostat/galvanostat. A 9 MHz AT-cut quartz crystal coated with gold was used as a working electrode. A decrease in frequency at this electrode corresponds to an increase in mass according to the Sauerbrey equation[11]

$$\Delta f = -C_f \Delta m \qquad (6)$$

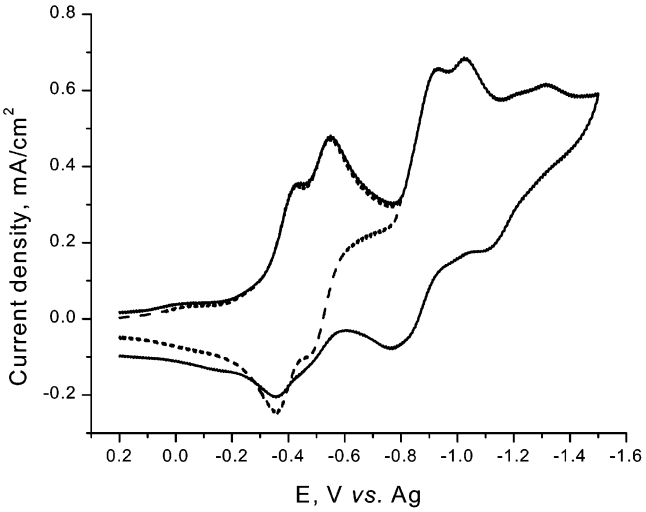

Figure 1. CVs for reduction of 1 mM CQ at a GC electrode in rigorously dried CH_3CN containing 0.10 M $TBAPF_6$ as a supporting electrolyte. The scan rate was 100 mV/s.

where Δf is the change in frequency, Δm is the mass change, and C_f is the sensitivity constant. The C_f value was obtained to be 6.68 ng/Hz/cm^2 from calibration experiments using silver deposition from a silver nitrate solution.

In situ UV−visible absorption spectra were taken with an Oriel InstaSpec IV spectrometer with a charge-coupled device (CCD) array detector, which was configured in a near normal incidence reflectance mode using a bifurcated quartz optical fiber.[12,13] A Xenone lamp (75 W) was used as a light source. The wavelength of the spectrograph was calibrated using a small mercury lamp.

Results and Discussion

Figure 1 shows typical cyclic voltammograms (CVs) of CQ in rigorously dried CH_3CN in an argon atmosphere. Similar results have been reported on electrochemical reduction of CQ in nonaqueous solutions such as CH_3CN,[7] DMF,[8] and CH_2Cl_2.[9] The CVs shown in Figure 1 are very similar to that described by Gomez-Kaifer et al.[7] except that the reduction waves are a little more reversible and better resolved in our case. These investigators attributed each CV wave to reduction of each *p*-BQ unit to form an anion radical. Thus, the first four waves shown in Figure 1 must be responsible for the consecutive formation of anion radicals of four *p*-BQ units, and the two following less reversible ones after the initial four waves should be further reduction of two of those anion radicals to corresponding dianions. The dianions are more reactive and the reversibility of the last two waves are significantly reduced compared to the first four waves. The difference in peak potentials between the second and third waves are significantly larger than those between the first and second as well as the third and fourth waves, indicating that the first two electron transfers take place at the first and third *p*-BQ units. The third electron transfer, however, occurs at the third *p*-BQ molecule, which is located between the two *p*-BQ anion radicals, resulting in a large resistance to the incoming electron. This explains why the potential differences between the first and second waves, as well as the third and fourth waves, are smaller than that between the second and third waves. After cycling the potential a few times, the working electrode was passivated due perhaps to the low solubility of reduced products formed from following chemical reactions of anion radicals and dianions of CQ (vide infra).

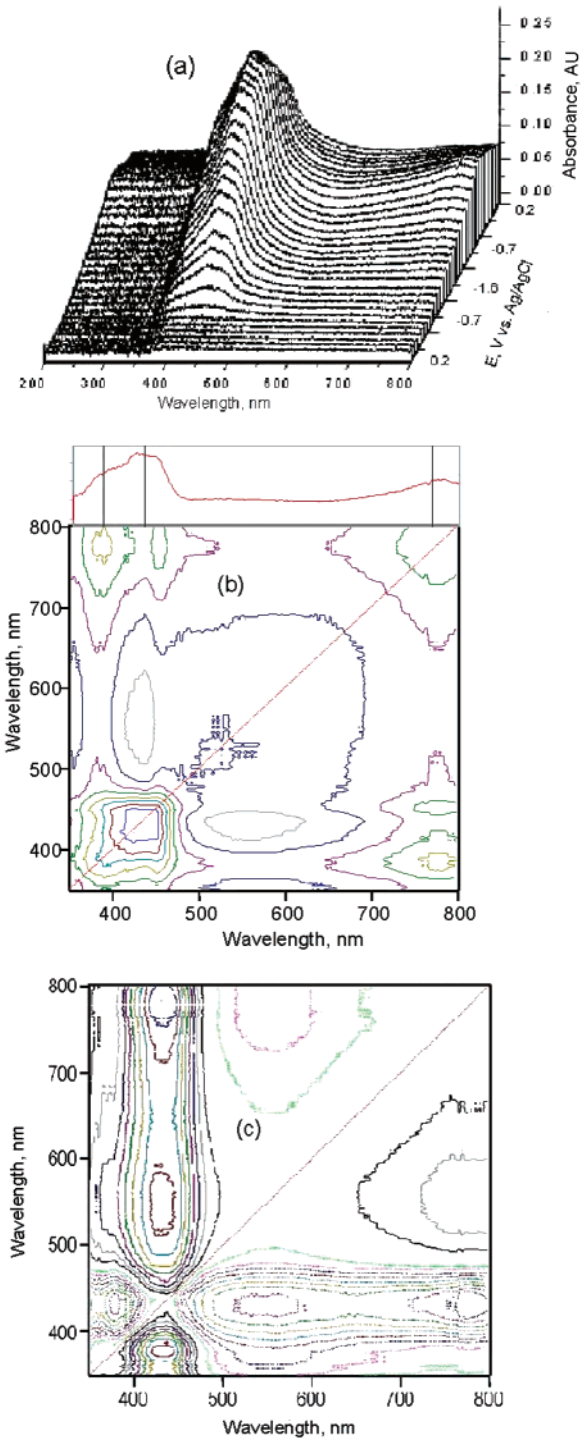

Figure 2. (a) In situ UV−vis absorption spectra recorded for reduction of 1.0 mM CQ by scanning between 0.2 and −1.6 V at a GC electrode in CH_3CN with 0.1 M $TBAPF_6$ at a scan rate of 100 mV/s. (b) Synchronous and (c) asynchronous 2D correlation contour maps of CQ. The dotted line indicates regions of negative correlation

To show that the four reduction waves do indeed result from the generation of anion radicals of *p*-BQ units, we carried out in situ spectroelectrochemical experiments. Figure 2 shows a series of in situ UV−vis absorbance spectra simultaneously obtained during reduction of 1.0 mM CQ by scanning the potential from +0.20 to −1.60 V at a reflective glassy carbon electrode in dry CH_3CN with 0.10 M $TBAPF_6$ used as a supporting electrolyte. Since the reference absorbance spectrum was taken at 0.20 V before the potential sweep started under otherwise identical conditions, the spectra obtained represent the differences in absorbance arising from the electrochemical reaction during the potential cycling. A relatively broad absorbance peak at around 436 nm with its shoulders ranging from 350 to 500 nm grows as CQ is reduced until another broad band begins to appear at bout 775 nm at a more negative potential. It is not clear, however, whether other absorption bands emerge as the potential becomes negative. For this reason, we ran two-dimensional (2D) correlation analysis to resolve and identify the absorption bands.[14] In the 2D-analysis method, synchronous and asynchronous spectra are obtained by applying a correlation analysis on a series of spectra obtained using an external perturbation such as changing potentials; synchronous spectra represent the overall similarity between two separate spectral intensity variations, whereas asynchronous spectra show the measure of dissimilarity of the spectral intensity variations.[14c] Because of the wide range of applications of this technique, it has become one of the standard analytical techniques for interpreting various types of spectroscopic data. The details are described elsewhere,[14] and no further description is given here. The synchronous 2D correlation spectrum obtained during the reoxidation of reduced CQ is shown in Figure 2b as a contour map. The intensity of a synchronous 2D correlation spectrum represents the simultaneous or coincidental changes of spectral intensity variations measured at two different wavelengths, ν_1 and ν_2. A power spectrum extracted along the diagonal line of the synchronous spectrum is also shown at the top of Figure 2b. Three autopeaks located at the diagonal line are clearly observed at 389, 436, and 775 nm, which are not readily detected in 1D spectra (Figure 2a). All cross-peaks located at off-diagonal line have positive signs indicating that these absorption peaks increase together. There are three autopeaks at 389, 436, and 775 nm, which also show up as cross-peaks as well. These cross-peaks show positive signs indicating that the absorbance peaks increase together.

The asynchronous 2D correlation spectrum shown in Figure 2c shows that the corresponding bands are occurring at different rates. An asynchronous cross-peak develops only if the intensities of two spectral features change out of phase (i.e., delayed or accelerated) with each other. The sign of an asynchronous cross-peak becomes positive if the intensity change at ν_1 occurs predominantly before ν_2 in the sequential order of perturbation. It becomes negative, on the other hand, if the change occurs after ν_2. This rule, however, is reversed if the synchronous peak is negative.[14] The analysis of the asynchronous spectrum indicates that the absorption bands emerge in the order of 436 → 389 → 775 → 550 nm. Further examination of the spectra singled out from those displayed in Figure 2a (not shown) reveals that the absorption peak at 436 nm increases monotonically until peaks at 389, 775, and 550 nm begin to show up when the potential becomes more negative than about −1.0 V, where dianions are produced. This leads to a conclusion that the band at 436 nm results from the first reduction product, i.e., anion radicals of *p*-BQ units. We thus assign the band at 436 nm to the anion radical, that at 775 nm to the free radical generated by protonation of the anion radical, i.e., $QH^{\bullet}$, and that at 550 nm to QH^- from the similarity of their wavelengths to those observed during electrolysis of *p*-BQ in DMSO in the presence and absence of water.[15,16] However, the band at 389 nm has not been reported in the literature, which we assign to the dianion, Q^{2-}, because it is observed only below −1.0 V. Here the $QH^{\bullet}$ band shows up after the dianion is generated because of the slow kinetics of the protonation reaction of $Q^{-\bullet}$ due to the trace amounts of protons available in the CH_3CN solution. The species QH^- would most likely be produced by

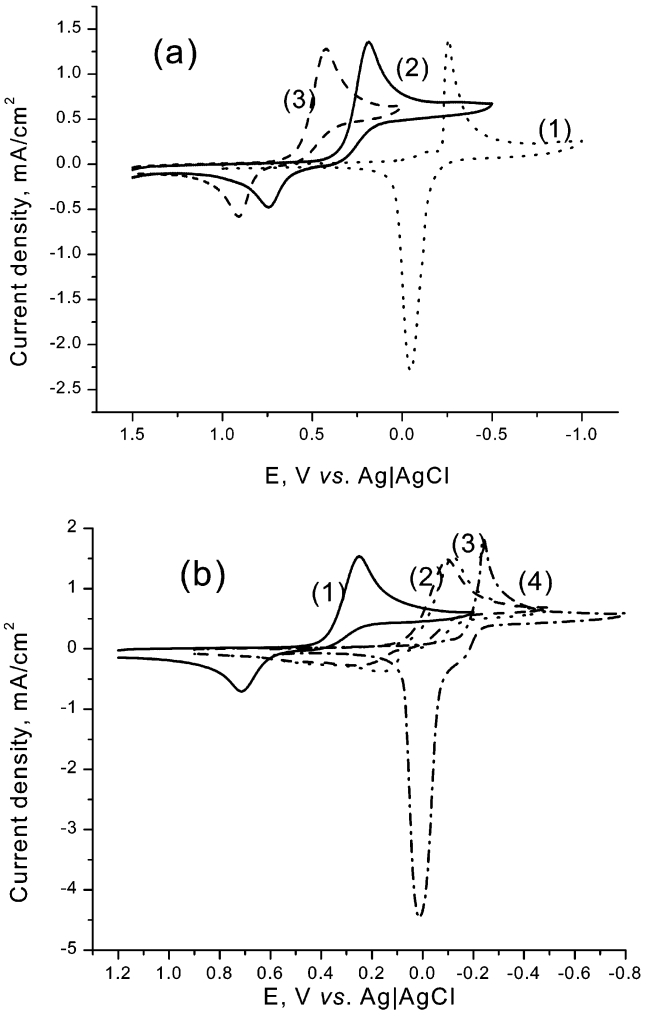

Figure 3. (a) CVs for reduction of 1.3 m*M* CQ with 2.2 M H_2O (1, ····), with 2.3 M H_2O and 62 mM $HClO_4$ (2, —), and with 62 mM $HClO_4$ and 0.14 M H_2O (3, ---) in CH_3CN with 0.1 M $LiClO_4$. The scan rate was 50 mV/s. (b) CVs for reduction of 1.3 m*M* CQ in an acetonitrile solution of 2.3 M H_2O and 0.1 M $LiClO_4$ with 62 m*M* of: (1) perchloric acid, (2) benzoic acid ($pK_a = 4.19$), (3) acetic acid ($pK_a = 4.75$), and (4) phenol ($pK_a = 9.98$). The working electrode was a GC disk for all of these measurements, and the scan rate was 50 mV/s and pK_a values are the dissociation constants in pure water at 20 °C.

protonation of Q^{2-} as well. Our spectroelectrochemical experiments provide clear evidence that the first four CV waves result from consecutive reduction of *p*-BQ upon potential sweep.

Since we obtained spectral information on intermediate species from the results in dry CH_3CN and yet the electrochemical reduction of CQ in aqueous media is of our primary interest, the next series of experiments were carried out in the presence of water. Because of the low solubility of CQ in water, we used acetonitrile as a major solvent with varied amounts of water and perchloric acid ($HClO_4$) as a proton donor.

Figure 3 shows CVs recorded for a 1.0 mM CQ solution in CH_3CN with 0.10 M $LiClO_4$ used as an electrolyte under various experimental conditions. Figure 3a shows CVs recorded in CH_3CN with (1) 2.20 M water only, (2) 2.34 M H_2O and 0.062 M $HClO_4$, and (3) 0.062 M $HClO_4$ and 0.14 M H_2O that came from $HClO_4$. A few comments can be made on these CVs. First, CVs shown here are significantly different from those obtained in dry CH_3CN in that a single peak is observed as opposed to a number of peaks observed in dry CH_3CN (Figure 1). Also, the CV behavior shown by CQ in the presence of water is entirely different from that of *p*-BQ in nonaqueous media with

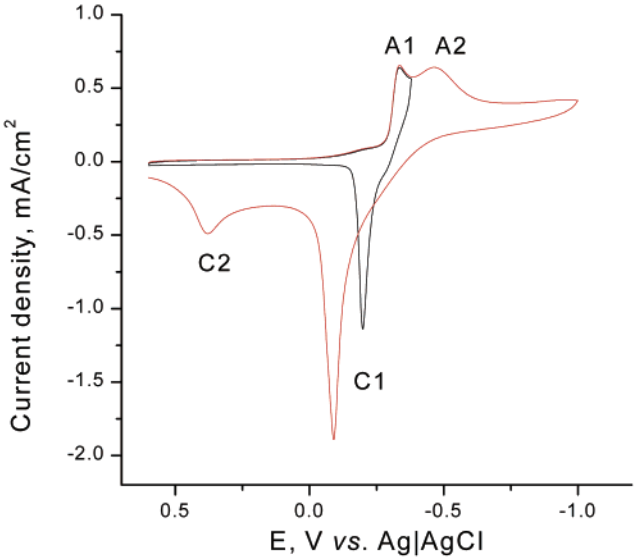

Figure 4. CVs recorded at a GC electrode for reduction of 0.50 mM CQ in a 0.10 M $LiClO_4$ solution in ACN containing 0.083 M H_2O at a scan rate of 50 mV/s.

water present (more will be discussed below). Second, the CV peak shows shifts in potential upon addition of proton donors such as $HClO_4$. This is an indication that the proton causes the following chemical reaction such as reactions 2 or 4 to the electrogenerated species.[17] Third, the current density is much larger in the presence of water than in its absence, indicating that more than just one electron transfer is taking place within a single CV peak. From the fact that the current density is increased drastically when water is added, we surmise that the series of reactions summarized by reactions 1−4 are indeed occurring within the single CV peak. Finally, the peak separation between the cathodic and anodic peaks is significantly different depending on whether there is an acid or not. The peak shift depends on the acidity of the proton donor (see curves 2 and 3). This is demonstrated clearly in CVs recorded in CH_3CN with different acid dissociation constants (Figure 3b). The peak separation is 212 mV without $HClO_4$ but 558 mV with the acid present. This indicates that the reversal (anodic) peak in the presence of acid is due to the reoxidation of the final product, perhaps CQH_8, whereas that with water alone is due to the reoxidation of intermediate species, which would not be the immediate reduction product, $CQ^{4-\bullet}$. This was confirmed by recording a CV for an authentic CQH_8 under identical experimental conditions (vide infra).

What appears to be a single CV peak when water is present is resolved when the amount of water is reduced or the scan rate is changed. Figure 4 shows CVs recorded in the presence of 0.083 M H_2O, in which the first and second CV peaks are clearly resolved due to the slow rate of protonation such that two electron transfer steps are resolved. Yet the current density is significantly larger than that shown in Figure 1. The peak separation between peaks A1 and C1 is only 137 mV, which becomes 245 mV when the potential is scanned down to −1.0 V. This indicates that the relatively slow chemical reaction proceeds following the electron transfer continuously to the final product, and eventually an intermediate species close to the final product is reoxidized at peak C2, if it is not the final product. Note also that the anodic peaks in both Figures 3 and 4 show characteristics of strong adsorption or precipitation. Thus, the product, regardless of whether it is an intermediate or final, is strongly adsorbed or precipitated on the electrode surface. More will be addressed on this below. The difference in CV shapes

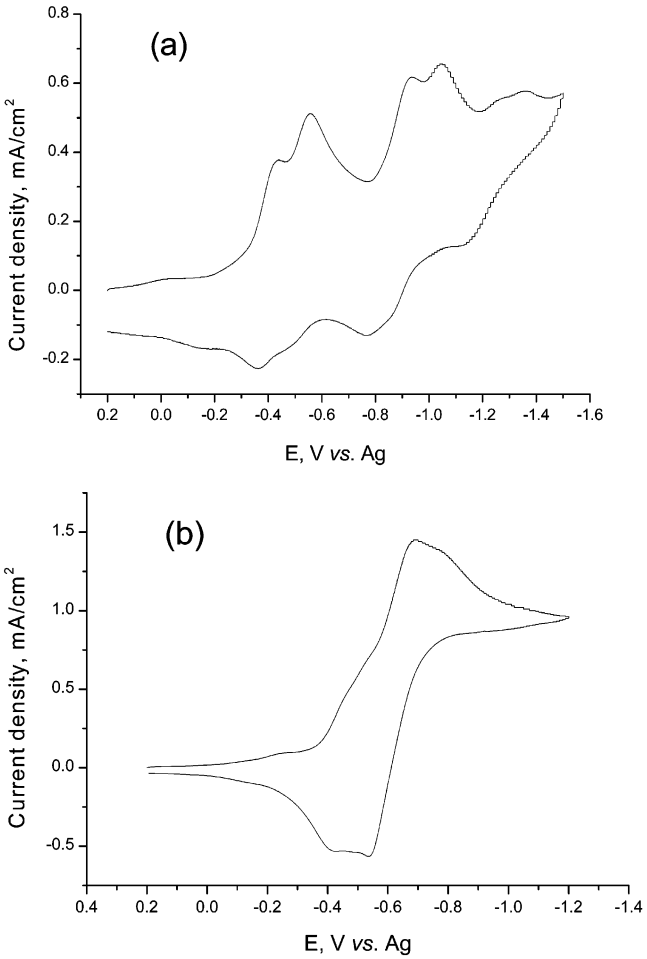

Figure 5. CVs recorded at a GC electrode for 0.90 mM CQ in a 0.10 M $TBAPF_6$ solution in ACN: (a) without and (b) with 2.20 M H_2O added. The scan rate was 50 mV/s.

shown in Figure 3a1 and that in Figure 5b indicates that the products, whether they are intermediate or final, are more soluble in a solution containing $TBAPF_6$ than in that having $LiClO_4$. In other words, a larger organic supporting electrolyte such as $TBAPF_6$ acts as a better surfactant for organic products than their more hydrophilic counterpart such as $LiClO_4$.

To see if indeed the ECEC reaction occurs within the single CV peak, we now compare the CVs recorded in CH_3CN without (a) and with (b) water under otherwise identical experimental conditions in Figure 5. The CVs show that the wave is more drawn out in this partially aqueous solution, and the ratio of the charges passed in the same potential range of +0.20 to −0.771 V, where the second peak hits its minimum just before its increase for the third peak in the absence of water, with and without water is about 2.1 for each electron transferred, indicating that the ECEC reactions must be occurring in a single CV peak. Note that $TBAPF_6$ was used as a supporting electrolyte to record CVs shown in Figures 1 and 5, while $LiClO_4$ was used for the rest of the experiments. This is because $LiClO_4$ was not used in rigorously dried solvents due to the difficulty of removing hydrated water, whereas $TBAPF_6$ had a solubility problem in a medium with a high water content.

To see how the water molecules interact with a CQ molecule, we carried out the water concentration dependency of CQ reduction in CH_3CN containing 62 mM $HClO_4$, and the result is shown in Figure 6. Since the peak potential shifts in a negative direction as the water concentration increases, water molecules

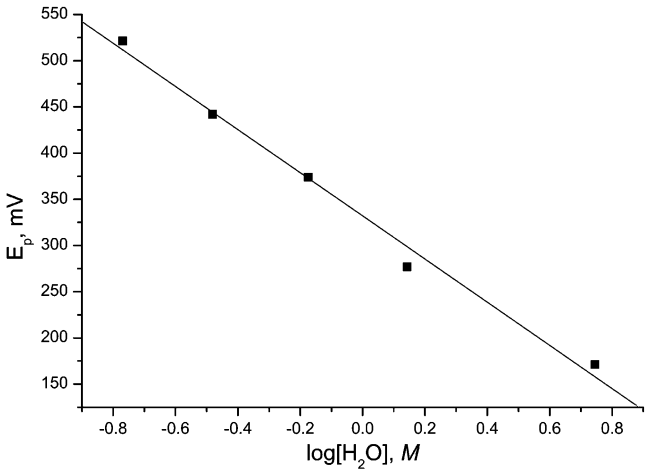

Figure 6. Correlation between E_p and log[H_2O] for the reduction of 0.50 m*M* CQ in an acetonitrile solution of 62 mM $HClO_4$ and 0.10 M $LiClO_4$.

must be chelating the CQ molecules as a result of an equilibrium reaction

$$CQ + pH_2O \rightleftharpoons CQ(H_2O)_p \tag{7}$$

which has a formation constant

$$K_f = \frac{[CQ(H_2O)_p]}{[CQ][H_2O]^p} \tag{8}$$

Based on eq 7, one can derive an equation

$$E_p = E_p{}^0 - \frac{RT}{nF}\ln(K_f) + \frac{mRT}{nF}\ln[H^+] + \frac{RT}{nF}\ln(CQ(H_2O)_p] - \frac{pRT}{nF}\ln[H_2O] \tag{9}$$

for an electron-transfer reaction

$$CQ + mH^+ + ne^- \rightleftharpoons CQH_m \tag{10}$$

Here $E_p{}^0$ is the peak potential for reaction 10 when no water is present in a 62 mM $HClO_4$ solution in CH_3CN, and E_p is the peak potential with water present. Equation 9 explains the decrease in peak potential for an increase in [H_2O] assuming that the addition of water does not change the proton concentration. The assumption is not unreasonable as $HClO_4$ is a strong acid and its ability to protonate the solvent would not be affected by the concentration of water. From the slope of the plot, we obtain a p/n value of 4.0 with a K_f value of 1.8×10^{20}. Thus, eight water molecules would be incorporated into each *p*-BQ unit.

To find if water molecules incorporated are charged, effects of the ionic strength have been studied by varying the concentration of $LiClO_4$ and the result is shown in Figure 7. As can be seen, the current for CQ reduction decreases as the ionic strength increases for a solution containing 0.50 mM CQ, 62 mM $HClO_4$, and varied amounts of $LiClO_4$. The decrease in current upon increase in ionic strength indicates that the electroactive species undergoing the reaction is an ionic species as its activity coefficient is affected by the ionic strength. Since an experiment cannot be run at the zero ionic strength, no standard state is available in this set of experiments, and there is no way of knowing the actual activity coefficient. Although we have no experimental information as to the charge of the

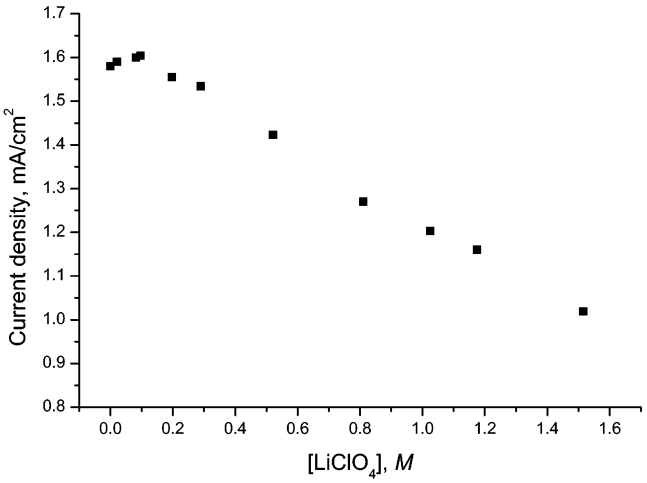

Figure 7. Plot of i_p vs [$LiClO_4$] for reduction of 0.50 m*M* CQ in an acetonitrile solution containing 62 mM $HClO_4$ and 2.30 *M* H_2O.

ionic species and, thus, on whether four water molecules are all or partially protonated, our experiments allow us to conclude that protonated water molecules are acting as ligands for each *p*-BQ during the reduction. This is partially supported by a recent theoretical work[18] wherein Q^{2-} shows a significant charge transfer to the hydrating water molecules. Since this charge transfer increases with an increasing number of water molecules, it is expected that Q^{2-} would give a full electron to neighboring water molecules in the presence of eight water molecules, resulting in Q^{-}−water or Q^{2-}−protonated water in the presence of proton sources.

From the results described thus far, the electrochemistry of CQ in *dry* CH_3CN can be regarded as an extension of that of *p*-BQ as can be seen from results shown in Figures 1 and 2, whereas its electrochemistry in the presence of water is entirely different from that of *p*-BQ in aqueous media. *p*-BQ undergoes a reversible one-electron transfer to form an anion radical upon reduction in nonaqueous media containing a large amount of water and even in unbuffered aqueous solutions above pH 2.5.[15,16] Its electrochemistry in buffered aqueous media or in unbuffered solutions of pH lower than 2.5 is described as a chemically reversible, but electrochemically irreversible, two electron reaction according to reaction 5,[5,19,20] which is the basis for the so-called quinone electrode used for pH measurements. No intermediate species has been detected for reaction 5 on an electrochemical time scale including CV and/or chronoamperometry. However, we saw clearly that the electrochemistry of CQ in dried ACN is entirely different from that with water as seen from Figures 1 and 3. When the medium is strongly acidic, we observe a reaction similar to reaction 5, i.e.

$$CQ + 8H^+ + 8e^- \rightleftharpoons CQH_8 \qquad (11)$$

On the other hand, the intermediate species, which suggest that the overall reaction consists of the elementary reactions given as (1)−(4), are detected in the CH_3CN solutions with just water alone or in mildly acidic solutions. Thus, the rate of the reaction sequence is slow enough for the intermediate species to be observed (Figure 4). One reason for the higher stability of the intermediate species generated during CQ reduction is because the reaction products such as $QH^{-\bullet}$, $QH^{\bullet}$, and QH^- freeze in the solid phase on the electrode surface as soon as they are produced. To show that this is the case, a series of microgravimetric experiments have been conducted using an EQCM technique.

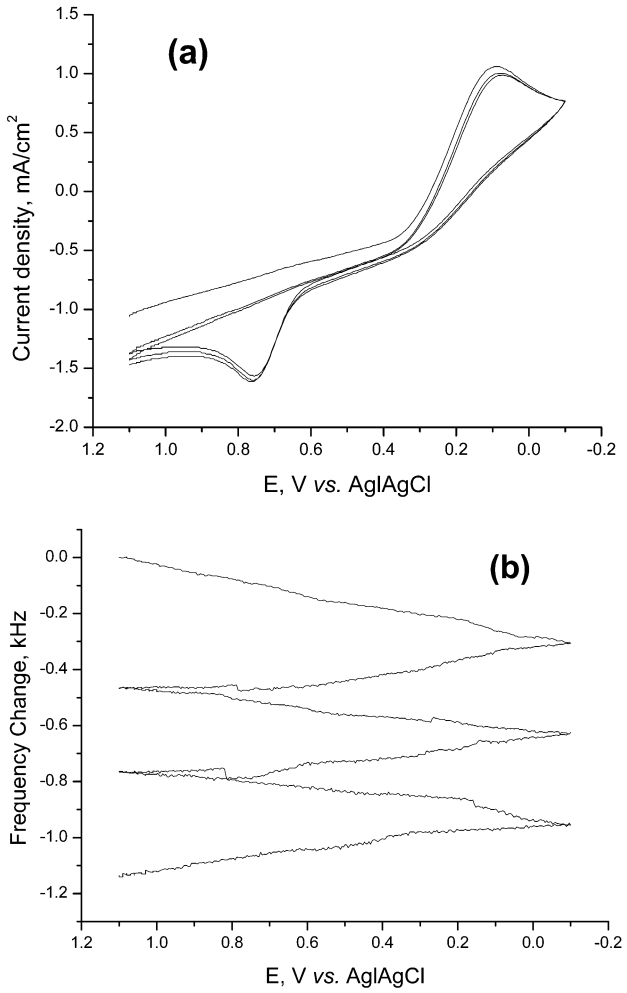

Figure 8. (a) Three consecutively recorded CVs at a Au-coated QCA electrode in a CH_3CN solution of 2.3 M H_2O, 62 mM $HClO_4$, 0.10 M $LiClO_4$, and 1.2 mM CQ; (b) Frequency shifts concurrently recorded with the CVs in (a). The scan rate was 50 mV/s.

Figure 8 shows CVs and frequency changes concurrently recorded during CQ reduction in a CH_3CN solution containing 62 mM $HClO_4$ and 2.3 M H_2O for the first three consecutive cycles at a gold coated quartz crystal electrode. Here CQ is reduced to CQH_8 according to reaction 11. The CV shown in Figure 8 is essentially identical to that shown in Figure 3a2 except that there is a large ohmic voltage drop (I·R drop) in the cell used for EQCM measurements due to its nonideal cell configuration compared to a normal cell used for Figure 3. Because of the I·R drop, the CV shown in Figure 8 is significantly sloped, and the peak separation became sizably larger than that shown in Figure 3a2. Also, the CV recorded from CQH_8 was essentially the reverse of that shown in Figure 8, indicating that reaction 11 is chemically reversible but electrochemically irreversible. This is another evidence that CQH_8 is produced when CQ is reduced in an organic medium containing a proton source. While CQ is being reduced to CQH_8, the accumulation of the product, CQH_8, on the electrode surface is shown by decreases in the frequency. The decrease of ∼400 Hz/cycle is relatively small perhaps because much of CQH_8 electrogenerated is dissolved as soon as it is produced. The amount precipitated is only about 15∼20% of that theoretically estimated from reaction 11. This is also shown by smaller anodic waves in comparison to cathodic waves at both the glassy carbon and gold electrodes [Figure 3a curves 2 and 3, and Figure 3b curve 1) and the gold electrode (Figure 8a)]. Even after the

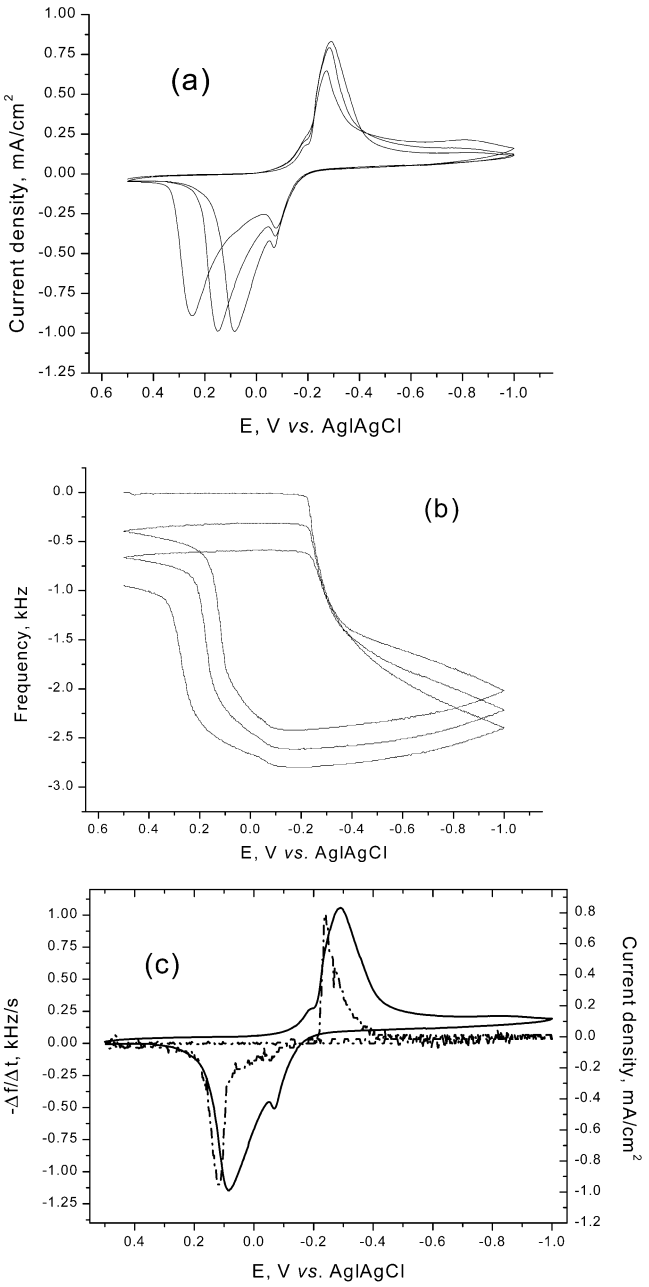

Figure 9. (a) Series of CVs at a gold-coated QCA electrode for three consecutive potential cycles in a CH_3CN solution of 2.2 M H_2O, 0.1 M $LiClO_4$, and 1.2 mM CQ; (b) Frequency shifts concurrently recorded with the CVs in (a); (c) CV and derivative signals of the frequency shift with respect to time vs voltage obtained from the first potential cycle shown in (a) and (b) above. The broken line indicates the -dΔf/dt signal while the solid line is the CVs. The scan rate was 50 mV/s.

anodic peak is past, no further weight decrease is observed, indicating that the dissolution is not caused by reoxidation of CQH_8.

Figure 9 shows the first three consecutive CVs (a), corresponding frequency changes (b), and the derivative signal of the frequency shift with respect to time (c), recorded in a CH_3CN solution containing only 2.2 M H_2O. As the potential cycling is continued, both the cathodic and anodic peak currents decrease and the second anodic peak shifts in a more positive direction. The CVs shown here are different from those shown previously in that two anodic peaks are resolved instead of the one observed at glassy carbon electrodes (Figure 3). Even at the GC electrode, well resolved CVs were often obtained (Figure 4). We found that the separation of the two anodic peaks has to do with the scan rate, indicating that different intermediate species may be detected depending on how much time has been allowed after the first electron transfer. In the present case, the electrochemical annealing of the reaction products by cycling repeatedly produces different states of the precipitate such as different crystalline forms or hydration numbers, which would cause the potential shifts.

Two features noticed from Figure 9b are (1) much larger amounts of insoluble products are precipitated initially on the surface than those shown in Figure 8b upon CQ reduction, but (2) a large fraction (~80%) of the initial precipitate is redissolved upon reoxidation as can be seen from the large frequency increase. This observation suggests that the intermediate species are more insoluble than the final product, CQH_8.

In efforts to see how the rate of precipitation/dissolution corresponds to its current counterpart, a derivative signal (dΔf/dt) obtained for the frequency change during the first cycle is shown in Figure 9c along with the concurrently recorded CV. In an ideal situation, where the electrogenerated products precipitate immediately on the electrode surface, the two signals should be identical.[11,21] In our case, the two signals are quite different, indicating that the electron transfer reaction does not straightforwardly lead to precipitation. Also, it is seen that the precipitation is delayed more during the anodic wave. That the dΔf/dt signal shows a slight delay behind the CV rise during the cathodic scan indicates that the intermediate species generated upon first electron transfer, most likely $QH^{\bullet}$, precipitates almost immediately, and the intermediate thus precipitated undergoes the following chemical and electron transfer reactions. In other words, the second and following electron transfers as well as chemical reactions take place inside the solid phase on the electrode after the first reduction product is rapidly adsorbed. We thus believe that further reactions to QH^- and QH_2 proceed within the solid phase. This must be the reason the overpotentials for the second and third steps are reduced so that only one broad peak appears. Also, this is why the limiting currents are reduced drastically to only about 1/7 ~ 1/6 of the peak current because the current is now controlled by the diffusion of CQ molecules and protons through the newly formed solid phase.

Upon reversing the potential, the dissolution of electrogenerated products upon anodic scan occurs only after nearly all of the anodic current has decayed. We assign the anodic peak at a more negative potential to the reoxidation of QH^- to $QH^{\bullet}$ and the second anodic peak following it to the oxidation of $QH^{\bullet}$ back to CQ. Depending on how long the products have been electrochemically annealed, the compactness of the solid phase and the physical and chemical transformations of the resulting precipitate, would differ, resulting in further potential shifts (Figure 9a). Part of the precipitate dissolves back into solution when the electrogenerated products are oxidized back to CQ. However, there still are some intermediate species and perhaps CQH_8 left on the surface because reoxidation of the reduced products requires the diffusion of protons toward the solution, which limits the reaction, and thus, part of CQH_8 remains on the surface. This explains why the dissolution of the precipitate from the electrode surface does not take place until all the anodic current has decayed in Figure 9c.

As already pointed out, an important difference between the electrochemical behaviors of *p*-BQ and that of its cyclic oligomer, CQ, in wet nonaqueous solutions arises from the fact that the intermediate species of *p*-BQ, i.e., $QH^{\bullet}$ and QH^-, are soluble, whereas the corresponding intermediate species of CQ

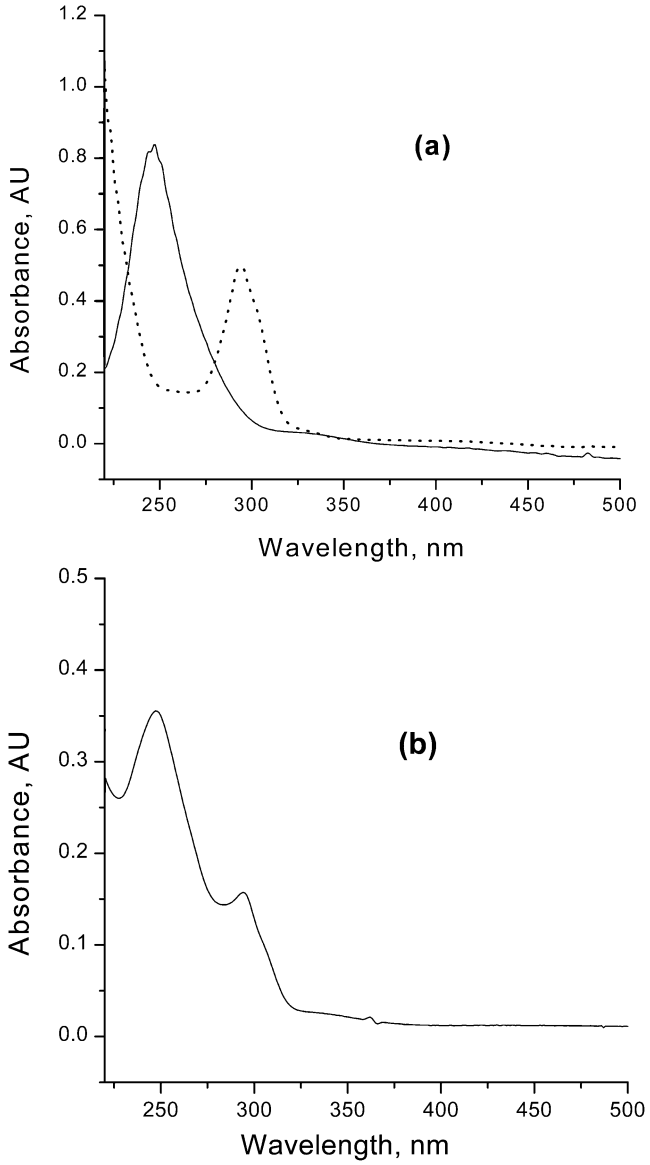

Figure 10. (a) UV−vis absorption spectra obtained in CH_3CN containing 2.2 M H_2O with authentic samples of 2.1×10^{-5} M CQ (solid line) and 3.3×10^{-5} M CQH_8 (dotted line), respectively; and (b) UV−vis absorption spectrum obtained after electrolysis of 1.0 mM CQ at 0 V for 90 min in the CH_3CN solution containing 2.2 M H_2O, 62 mM $HClO_4$, and 0.1 M $LiClO_4$. The working electrode was a Pt wire with Ag/AgCl and Pt gauze used as reference and counter electrodes, respectively.

reduction are not. This explains why the electrochemistry of CQ is not a simple extension of that of *p*-BQ.

To detect the intermediate species, we ran in situ spectroelectrochemical experiments. Figure 10 shows (a) the absorption spectra of authentic samples of CQ and CQH_8 in a 2.2 M H_2O solution in CH_3CN and (b) the in situ absorption spectrum obtained during the electrolysis of 1 mM CQ in a wet CH_3CN solution with $HClO_4$ at a reflective glassy carbon working electrode. It is seen clearly that the only product upon electrochemical reduction of CQ in wet CH_3CN containing $HClO_4$ is CQH_8 as was expected; the spectrum shown in Figure 10b is just made of the mixture of CQ and CQH_8 in solution. The CQH_8 peak absorbing at 296 nm is overlaid on the shoulder of the absorption peak of CQ at 247 nm.

Figure 11a shows a series of in situ absorption spectra recorded during a potential sweep in a wet CH_3CN solution of 1.0 mM CQ and 2-D correlation spectra obtained from them

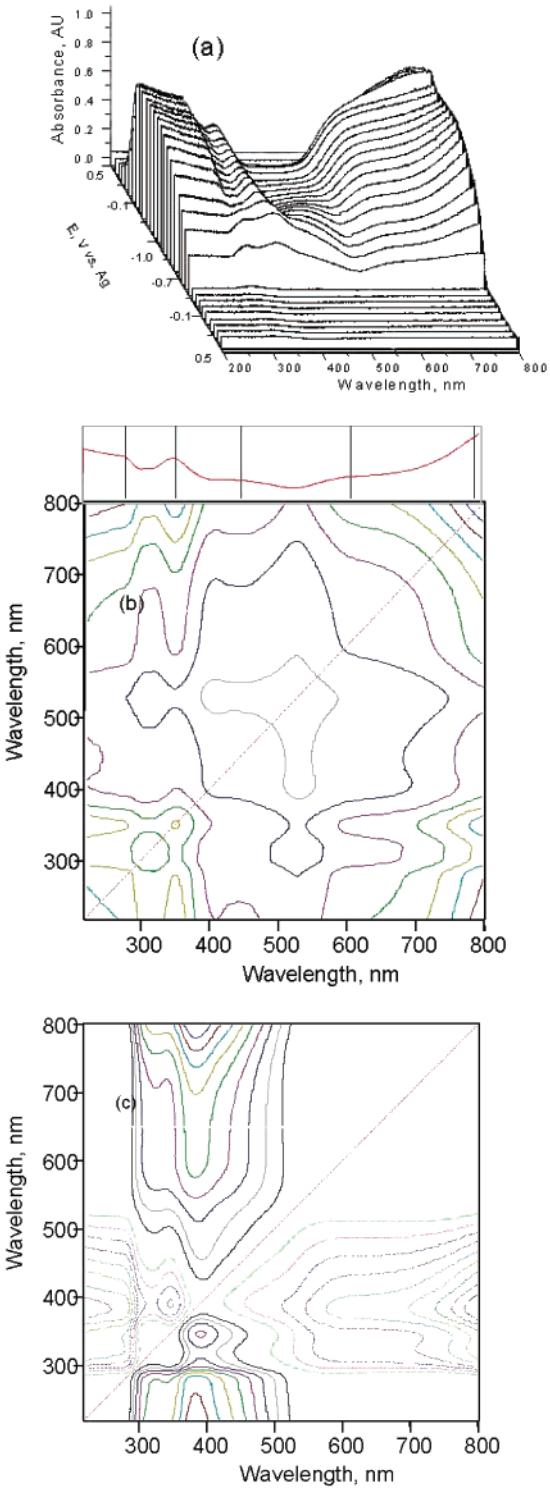

Figure 11. (a) In situ UV−vis absorption spectra recorded at a reflective glassy carbon electrode during potential cyc1es between 0.5 and −1.0 V in CH_3CN with 2.2 M H_2O, 0.10 M $LiClO_4$, and 1.2 mM CQ. The scan rate was 50 mV/s; (b) Synchronous and (c) asynchronous 2D correlation contour maps of derived from spectra shown in (a). The dotted line indicates regions of negative correlation.

(Figure 11, parts b and c). There are a number of absorption bands with their intensities varying during the potential sweep, which are difficult to identify or resolve. For this reason, we ran 2D analyses, and the 2D synchronous and asynchronous correlation spectra are shown in Figure 11, parts b and c. The synchronous spectrum identifies four auto peaks at 282, 391, 452, and 788 nm. The signs of cross-peaks of the synchronous

spectrum are all positive, indicating that they all grow during the negative potential scan. Analysis of the asynchronous 2D correlation spectrum indicates that the band at 595 nm occurs at about the same time as that at 282 and 788 nm after the peaks at 391 and 452 nm show up first. Thus, the peaks at 282, 595, and 788 start to emerge at about the same time after the absorption peak at 391 nm has shown up first, followed by that at 452.

All of the absorption bands identified here were also present in the spectra obtained in dry CH_3CN except for the band at 282 nm, though all of the bands are red or blue shifted compared to those observed in dry CH_3CN shown in Figure 2 and those shown in Figure 10. We believe relatively large spectral shifts observed here are due primarily to poor spectral resolution ($\sim$0.4 nm at 546 nm) as a result of a relatively wide slit width used (25 μm) for a higher spectral sensitivity and also heavy spectral overlaps of broad absorption peaks resulting from the generation of large amounts of intermediate species, most of which absorb light in a broad spectral region. Accepting this, we assign the 282 nm peak to CQH_8, 391 nm to CQ^{2-}, 452 nm to $CQ^{-\bullet}$, 595 nm to CHQ^-, and 788 nm to $CHQ^\bullet$ in reference to our earlier assignments for the bands in spectra obtained in dry CH_3CN. The sequence of the band emergence is also very revealing. The appearance of the 391 nm band (CQ^{2-}) first in the series must be due to the fact that the last protonation step to produce the CQH_8 is the slowest rate-limiting step of the whole CQ reduction reactions in the presence of water. The emergence of the 452 nm band ($Q^{-\bullet}$) next in the series indicates that the protonation of the anion radical is the second slowest step and begins to be populated a little after the electrolysis begins. Finally the fact that $CHQ^\bullet$ and CHQ^- appear last in the series along with CQH_8 indicates that further reduction of $CHQ^\bullet$ to CHQ^- and its protonation to produce the final product CQH_8 is relatively fast. Only after all of these series of reactions proceed, the final product, CQH_8, is produced.

Our assignments here for the results obtained from the two extremes of the spectroelectrochemical experiments conducted without water (Figure 2) and with water (Figure 11) are consistent with each other. These results show indeed that the reaction is taking place via the elementary reaction steps summarized by reactions 1 through 4. The fact that the sequence of absorption band emergence is different in dry and wet CH_3CN indicates that the reaction rates are modulated by the presence of a reactant such as proton as well as its concentration. Although the spectroelectrochemical experiments do not provide information on reaction kinetics, it certainly gives clues to the identification of the rate-limiting step, which should be a starting point for computer simulation of the currents to evaluate the related rate constants.

Conclusions

The electrochemical reduction of CQ in CH_3CN with and without water and/or $HClO_4$ has been investigated using electrochemical, EQCM, and spectroelectrochemical techniques. CQ undergoes consecutive four one-electron transfer reactions, followed by further reduction to dianions in rigorously dried CH_3CN. This was demonstrated by spectra recorded during the potential sweep, in which the spectrum of one species increases until after the fifth and sixth CV peaks are observed, where the formation of the most reactive species, dianions, is detected.

The results obtained in dry CH_3CN provided the basis to the interpretation of the electrochemistry of CQ in CH_3CN containing water and/or $HClO_4$. When CQ is electrochemically reduced in CH_3CN in the presence of a strong acid such as $HClO_4$, a concerted eight-electron reduction to the final product, CQH_8, is obtained similar to reaction 5 as would be expected from the electrochemistry of its monomeric counterpart, *p*-BQ. It was also found that the CQ reduction potential shows an acidity dependency, indicating that the proton accelerates the following chemical reaction after the electron transfer. The water concentration dependency of the CQ reduction potential and the ionic strength dependency of the reduction current in the presence of $HClO_4$ led us to conclude that protonated water molecules interact with the CQ molecule by forming a complex whose formation constant is 1.8×10^{20}.

The results obtained from the EQCM and spectroelectrochemical experiments show that CQ reduction in CH_3CN containing just 2.2 M water undergoes a series of ECEC reactions to eventually produce the final product, CQH_8. The EQCM measurements indicate that what appears to be a single CV peak actually consists of a series of electron transfer and following chemical reactions. The final product, CQH_8, and all of the intermediate species produced during the electrolysis of CQ in dry CH_3CN are detected in the spectra recorded during the electrolysis in wet CH_3CN.

It has been reported that CQH_8 is known to form organic nanotubes via four hydrogen bonds formed between OH groups of hydroquinone (HQ) moieties and water molecules.[4] It is for this reason that the electrochemical reduction of CQ is important as a good understanding of its mechanism would allow the various parameters for CQ reduction and thus the tube formation to be straightforwardly controlled. In fact, our present results suggest that CQ is already in the form, which would lead to the tubular structure upon reduction. Our preliminary results show that relatively large nanotubes are formed upon CQ reduction, and studies to fine-tune this reaction are currently under way in our laboratory. In addition, the exploitation of structural changes from CQ (partial cone shape) to CQH_8 (cone shape) or vice versa could be utilized to design a novel electrochemically controllable nanomechanical devices, like those of quino-cyclophane systems.[22]

Acknowledgment. This work was supported by a grant from the Korea Science and Engineering Foundation (KOSEF) through the Center for Integrated Molecular Systems, Pohang University of Science and Technology. The graduate stipends for Y.O.K. were provided through the BK 21 program by the Ministry of Education of Korea.

References and Notes

(1) Gutsche, C. D. *Calixarenes*; The Royal Society of Chemistry: Cambridge, U.K., 1989.

(2) Reddy, P. A.; Gutsche, C. D. *J. Org. Chem.* **1993**, *58*, 3245.

(3) (a) Kelderman, E.; Derhaeg, L.; Heesink, G. J. T.; Verboom, W.; Engbersen, J. F. J.; van Hulst, N. F.; Persoons A.; Reinhoudt, D. N. *Angew. Chem., Int. Ed. Engl.* **1992**, *31*, 1075. (b) Verboom, W.; Durie, A.; Egberink, R. J. M.; Asfari Z.; Reinhoudt, D. N. *J. Org. Chem.* **1992**, *57*, 1313.

(4) (a) Hong, B. H.; Bae, S. C.; Lee, C.-W.; Jeong, S.; Kim, K. S. *Science* **2001**, *294*, 348. (b) Hong, B. H.; Lee, J. Y.; Lee, C.-W.; Kim, J. C.; Kim, K. S. *J. Am. Chem. Soc.* **2001**, *123*, 10748. (c) Kim, K. S.; Suh, S. B.; Kim, J. C.; Hong, B. H.; Lee, E. C.; Yun, S.; Tarakeshwar, P.; Lee, J. Y.; Kim, Y.; Ihm, H.; Kim, H. G.; Lee, J. W.; Kim, J. K.; Lee, H. M.; Kim, D.; Cui, C.; Youn, S. J.; Chung, H. Y.; Choi, H. S.; Lee, C.-W.; Cho, S. J.; Jeong, S.; Cho, J.-H. *J. Am. Chem. Soc.* **2002**, *124*, 14268.

(5) Patai, S.; Rappoport, Z. *The Chemistry of the Quinonoid Compounds*; Wiley: New York, 1974.

(6) (a) Turner, W. E.; Elving, P. T. *J. Electrochem. Soc.* **1965**, *112*, 1215. (b) Eggins, B. R.; Chambers, J. Q. *J. Electrochem. Soc.* **1970**, *117*, 186. (c) Koshy, V. J.; Sawayambunathan, V.; Periasamy, N. *J. Electrochem. Soc.* **1980**, *127*, 2761.

(7) Gomez-Kaifer, M.; Reddy, P. A.; Gutsche, C. D.; Echegoyen, L. *J. Am. Chem. Soc.* **1994**, *116*, 3580.

(8) Suga, K.; Fujihara, M.; Morita, Y.; Agawa, T. *J. Chem. Soc., Faraday Trans.* **1991**, *87*, 1575.

(9) Casnati, A.; Comelli, E.; Fabbi, M.; Bocchi, V.; Mori, G.; Ugozzoli, F.; Manotti-Lanfredi, A. M.; Pochini, A.; Ungaro, R. *Recl. Trav. Chim. Pays-Bas* **1993**, *112*, 384.

(10) Morita, Y.; Agawa, T.; Nomura, E.; Taniguchi, H. *J. Org. Chem.* **1992**, *57*, 3658.

(11) Rubinstein, I. *Physical Electrochemistry*; Marcel Dekker: New York, 1995.

(12) Pyun, C.-H.; Park, S.-M. *Anal. Chem.* **1986**, *58*, 251.

(13) (a) Zhang, C.; Park, S.-M. *Anal. Chem.* **1988**, *60*, 1639. (b) Zhang, C.; Park, S.-M. *Bull. Korean Chem. Soc.* **1989**, *10*, 302.

(14) (a) Noda, I. *J. Am. Chem. Soc.* **1989**, *111*, 8116. (b) Noda, I. *Appl. Spectrosc.* **1990**, *44*, 550. (c) Noda, I.; Dowrey, A. E.; Marcott, C.; Story, G. M.; Ozaki, Y. *Appl. Spectrosc.* **2000**, *54*, 236A.

(15) Shim, Y.-B.; Park, S.-M. *J. Electroanal. Chem.* **1997**, *425*, 201.

(16) Pyun, C.-H.; Park, S.-M. *J. Electrochem. Soc.* **1985**, *132*, 2426.

(17) Gupta, N.; Linschitz, H. *J. Am. Chem. Soc.* **1997**, *119*, 6384.

(18) Manojkumar, T. K.; Choi, H. S.; Tarakeshwar, P.; Kim, K. S. *J. Chem. Phys.* **2003**, *118*, 8681.

(19) Bard, A. J.; Lund, H. *Encyclopedia of Electrochemistry of the Elements*; Marcel Dekker: New York, 1978; Vol. XII.

(20) Cantor, C. R. *Energy Transduction in Biological Membranes*; Springer-Verlag: New York, 1990.

(21) Lee, H. J.; Cui, S.-Y.; Park, S.-M. *J. Electrochem. Soc.* **2001**, *148*, D139.

(22) Kim, H. G.; Lee, C.-W.; Yun, S.; Hong, B. H.; Kim, Y.-O.; Kim, D.; Ihm, H.; Lee, J. W.; Lee, E. C.; Tarakeshwar, P.; Park, S.-M.; Kim, K. S. *Org. Lett.* **2002**, *4*, 3971.